Ultra-flexible organic field-effect transistors embedded at a neutral strain position

Tsuyoshi Sekitani, Shingo Iba, Yusaku Kato, Yoshiaki Noguchi, and Takao Someya*

Quantum Phase Electronics Center, School of Engineering, University of Tokyo

7-3-1 Hongo, Bunkyo-ku, Tokyo 113-8656, Japan

Takayasu Sakurai

Center for Collaborative Research, University of Tokyo,

4-6-1 Komaba, Meguro-ku, Tokyo 153-8505, Japan

We fabricated ultra-flexible pentacene field-effect transistors (FETs) with a mobility of 0.5 cm^2/Vs and an on/off ratio of 10^5, which are functional at the bending radius less than 1 mm. The transistors are manufactured on a 13-μm-thick polyimide film and covered by a 13-μm-thick poly-chloro-para-xylylene encapsulation layer so that transistors can be embedded at a neutral position. This sandwiched structure can drastically suppress strain-induced changes in transistor characteristics. Furthermore, the FETs show no significant change after bending cycles of 60,000 times on inward and outward bending stresses.

*Correspondence should be sent to someya@ap.t.u-tokyo.ac.jp

Organic field-effect transistors (FETs) have attracted much attention because they are suitable to realize mechanically flexible, lightweight, printable, and large-area electronics. Those attributes are very important to realize flexible electronics including paper-like displays [1,2] and flexible sensors such as artificial skins [3-5] and sheet scanner [6]. Although few works have been reported on mechanical flexibility of organic transistors, we have recently manufactured very flexible organic transistors with polyimide gate insulators and demonstrated that those transistors were functional at the bending radius (R) of the base film curvature down to 4.6 mm. We have also found in those transistors that strain changed mobility by 10 % at R~4.6 mm [7], which should be minimized to achieve reliable operation of bended organic integrated circuits.

In this work, we manufactured pentacene FETs on 13-μm-thick polyimide films with polyimide gate dielectric layers, which are encapsulated by passivation layers of poly-chloro-para-xylylene with same thickness as base films, and suppressed the strain-induced changes in transistor performance. With decreasing the bending radius down to 2 mm, the change in mobility is less than 3 %. Further decrease of the bending radius (R) causes systematic change in mobility. However, organic FETs are functional even at R down to 0.5 mm. The change in transistor characteristics is reversible and reproducible even when R is 0.5 mm.

A cross-sectional illustration of the present device is shown in Fig. 1 (a). A gate electrode (G) consisting of 5-nm-thick Cr as an adhesion layer and 100-nm-thick Au is deposited through a shadow mask in a vacuum evaporator on a 13-μm-thick polyimide film. Then, polyimide precursors are spin-coated to form 500-nm-thick gate dielectric layers [3,8]. A 50-nm-thick pentacene is deposited, and then 50-nm-thick Au drain (D) and source electrodes (S) are

evaporated. The channel length (L) and width (W) of the FETs are 100 μm and 1 mm, respectively. Finally, the base film with transistors is uniformly coated by a 13-μm-thick poly-chloro-para-xylylene (dix-SR, Daisankasei Co., Ltd.) passivation layer, hereafter referred to as a parylene layer. Therefore, the FETs are placed at the neutral position by sandwiching between a base film and an encapsulation layer. The direction of source-drain current paths is precisely arranged parallel to the direction of strain. A capacitor is also manufactured simultaneously on the same base film and its capacitance is measured while changing the bending radius of the base films in order to obtain precise capacitance of polyimide gate dielectric layers with bending stress. Furthermore, its characteristics of capacitor can function as a strain gauge. We measured electrical properties of the FETs under various inward and outward bending strains, whose magnitudes were systematically controlled with changing the bending radius (R) of the base plastic films. Schematic illustrations of inward and outward bending are shown in Fig. 2. These explanations in details including the experimental setup and methods of analysis for strain evaluated from bending radius have been reported previously [7].

Figure 1 (b) shows the typical DC characteristics of manufactured transistors measured at a light-shielding ambient environment before the start of bending experiments. We monitor a source-drain current (I_{DS}) of FETs as a function of source-drain voltage (V_{DS}): A gate voltage (V_{GS}) is changed from 20 to –40 V in –10 V steps. The evaluated mobility is as high as 0.5 cm^2/Vs in the saturation regime, and the on/off ratio exceeds 10^5.

We measure the transfer characteristics of the FETs under inward and outward bending strains, while changing the bending radius (R) of the base film, as shown in Figs. 2 (a) and (b).

Although inward and outward bending stresses down to 2 mm are applied to the devices, saturation currents show slight changes less than 2 % on both bending stresses. However, saturation current increases by 10 % and decreases by 25 % under the inward and outward bending radius down to 0.5 mm, respectively.

Figure 3 shows the mobility as a function of R. We apply inward or outward bending strains induced by reducing bending radius from flat (R=∞) to R=0.5 mm. With decreasing R down to 2 mm, the change in mobility is less than 3 % on both bending cases, which indicates that strain-induced changes in transistor performance are negligible small down to R=2 mm. This demonstrates that the present FETs have an excellent stability under strains. However, further decrease of R from 2 mm to 0.5 mm causes systematic changes in mobility, namely, it increases by 20 % on inward bending or decreases by 30 % on outward bending stress. Furthermore, the changes in transistor characteristics are reversible and reproducible even when R is 0.5 mm.

In order to investigate the recovery performance after stressing the FETs, a lot of inward and outward bending stresses (bending cycles) of R=2 mm are applied to the FETs. First, the FET is bend from flat (R=∞) to R=2 mm, and immediately released up to flat state. Again, the same FET is bend down to R=2 mm and released. This procedure is repeated on bending cycles of 110 times for a minute. Measurements are performed at each number of bending cycles with applications of voltage bias of V_{DS}=V_{GS}= - 40V, which should be distinguished from continuous DC bias stress. Figure 4 shows the normalized I_{DS} as a function of the number of outward bending cycles. There is no significant change even after bending cycles up to 60,000 times, while I_{DS} decreases after 60,000 times, and finally decreases by 10 % at 160,000 times. The

dependence of transistor performance under inward bending cycles is qualitatively the same. Such negligible changes in transistor characteristics under a lot of bending cycles have not yet been achieved in any other transistors including organic [3,7], single crystalline-silicon [9], and amorphous-silicon FETs so far [10-12].

Figure 5 shows the change in I_{DS} as a function of inward bending radius on organic FETs with different device structural parameters: a 13-μm-thick base film and a 13-μm-thick encapsulation layer (sample A), a 13-μm-thick base film and a 10-μm-thick encapsulation layer (sample B), and a 125-μm-thick base film and no encapsulation layer (sample C), where those FETs have a same thickness (500 nm) of polyimide gate dielectric layers. Inward bending stresses are corresponding to the compressive strain. Sample C shows a drastic decrease of I_{DS} at R=5 mm, at which irreversible degradations are observed (This R is defined as a critical bending radius), and strain-induced changes are observed at bending radii below 17 mm. However, sample A shows the critical bending radius of 0.5 mm, and strain-induced changes are seen only at bending radii below 3 mm. Sample B has a critical bending radius of 0.8 mm, which is larger than that of sample A. Even a subtle difference in the thickness of encapsulation layers can affect the strain-induced changes in performance; this reflects the accuracy of experiment.

As explained above, thinning base films and the structure sandwiched between a sealant and base film is effective in reducing the critical bending radius. Suo *et al*. reported a theoretical analysis of the strain on FETs embedded at the neutral position [10]. Loo *et al*. fabricated organic FETs placed near the neutral mechanical plane and achieved the critical bending radius of 7.5 mm [13].

We would like to highlight that the changes in the structural parameters, namely, L, W, and the thickness of gate dielectric layers, that occur with the application of strain can be reproduced well by the classical Poisson model [7]. In fact, the capacitance of polyimide dielectric layers decreases under a compressive strain and increases under a tensile strain. This change is completely consistent with the change in the thickness of polyimide layers caused by the Poisson effect.

When FETs have no encapsulation layers, inward bending of the base film induces compressive strains at a position of FETs, and outward bending induces tensile strains. On the other hand, encapsulation layers induce opposite strains at the same position. Therefore, FETs with encapsulation layers that have just the same thickness as the base films would not suffer from the bending stress.

Based on the simple multilayer model [14], the strain would be 0% if the FETs are placed at the neutral mechanical plane. Thus, it is expected that sample A can function even when R is less than 0.1 mm. However, our experimental results revealed that the critical bending radius for sample A is 0.5 mm. We speculate that this discrepancy between experiment and theory can be ascribed to the fact that the thickness of each layer of the organic transistor is very small, but finite. In fact, the thickness of the polyimide gate insulator is 500 nm; therefore, the channel layer is slightly strained. In order to theoretically reproduce our experimental results, an analysis that is more sophisticated than the simple multilayer model will be necessary, which is an important topic for future research.

We thank Kyocera Chemical Cooperation for providing high-purity polyimide precursors and Daisankasei Co., Ltd. for providing high-purity parylene. This study is partially supported by IT Program and TOKUTEI (15073204), MEXT, MPHPT, and NEDO.

REFERENCES

1. J. A. Rogers, Z. Bao, K. Baldwin, A. Dodabalapur, B. Crone, V. R. Raju, V. Kuck, H. Katz, K. Amundson, J. Ewing, and P. Drzaic, Proc. Natl. Acad. Sci. U.S.A. **98**, 4835 (2001).
2. C. D. Sheraw, L. Zhou, J. R. Huang, D. J. Gundlach, T. N. Jackson, M. G. Kane, I. G. Hill, M. S. Hammond, J. Campi, B. K. Greening, J. Francl, and J. West, Appl. Phys. Lett. **80**, 1088 (2002).
3. T. Someya, T. Sekitani, S. Iba, Y. Kato, H. Kawaguchi, and T. Sakurai, Proc. Natl. Acad. Sci. U.S.A. **101**, 9966 (2004).
4. H. Kawaguchi, T. Someya, T. Sekitani, and T. Sakurai, IEEE J. Solid-State Circuits. **40**, 177 (2005).
5. T. Someya, Y. Kato, T. Sekitani, S. Iba, Y. Noguchi, Y. Murase, H. Kawaguchi, and T. Sakurai, Proc. Natl. Acad. Sci. U.S.A. **102**, 12321 (2005).
6. T. Someya, S. Iba, Y. Kato, T. Sekitani, Y. Noguchi, Y. Murase, H. Kawaguchi, and T. Sakurai, Tech. Dig. IEEE International Electron Devices Meeting, 580 (2004).
7. T. Sekitani, Y. Kato, S. Iba, H. Shinaoka, T. Someya, T. Sakurai, S. Takagi, Appl. Phys. Lett. **86**, 073511 (2005).
8. Y. Kato, S. Iba, R. Teramoto, T. Sekitani, T. Someya. H. Kawaguchi, and T. Sakurai, Appl. Phys. Lett. **84**, 3789 (2004).
9. E. Menard, R. G.. Nuzzo, and J. Rogers, Appl. Phys. Lett. **86**, 093507 (2005).
10. Z. Suo, E. Y. Ma, H. Gleskova, and S. Wagner, Appl. Phys. Lett. **74**, 1177 (1999).
11. H. Gleskova, S. Wagner, W. Soboyejo, and Z. Suo, J. Appl. Phys. **92**, 6224 (2002).
12. S. H. Won, J. K. Kyun, C. B. Lee, H. C. Nam, J. H. Hur, and J. Jang, J. Electrochem. Soc. **151** (3), G167 (2004).

13. Y.-L. Loo, T. Someya, K. W. Baldwin, Z. Bao, P. Ho, A. Dodabalapur, H. E. Katz, J. A. Rogers, Proc. Natl. Acad. Sci. U.S.A. **99**, 10252 (2002).

14. The strain (S) at the FETs with a sandwich structure is described as $S = \left(\frac{d_f + d_s}{2R} \right) \frac{\left(1 + 2\eta + \chi\eta^2\right)}{(1+\eta)(1+\chi\eta)} - \left(\frac{d_e}{2R} \right)$, where R represents bending radius, d_f the thickness of a gate dielectric layer, d_s the thickness of a base film layer, and d_e the thickness of an encapsulation layer, $\eta = d_f/d_s$, $\chi = Y_f/Y_s$: Y_f and Y_s Young's modulus of a gate dielectric layer and a base film, respectively [10,11].

Figure captions

Figure 1: (a) The cross-sectional illustration of organic transistors on plastic films with polyimide gate dielectric layers and parylene passivation layers. (b) Source-drain current (I_{DS}) measured under ambient environment as a function of source-drain voltage (V_{DS}). A gate voltage (V_{GS}) is changed from 20 to – 40 V in – 10 V steps.

Figure 2: Transfer characteristics with bending radii of R=20, 10, 5, 2, 1, and 0.5 mm; which are corresponding to (a) inward and (b) outward bending strains. A V_{GS} is swept from 20 to –40 V with application of V_{DS} = – 40 V.

Figure 3: Mobility (μ) as a function of bending radius from 20 mm down to 0 mm. Right and left figures show inward and outward bending, respectively. Insets show the magnified view at the bending radius from 3 mm to 0.5 mm.

Figure 4: Normalized source-drain current as a function of the number of outward bending cycles (R=2 mm). The data are normalized by the start of the measurement. This procedure is repeated on bending cycles of 110 times for a minute, and measurements are performed with applications of V_{DS} = V_{GS} = - 40 V.

Figure 5: Change in source-drain currents as a function of bending radius (compressive strain) on organic FETs with different device structural parameters: (A) a 13-μm-thick base film with a 13-μm-thick encapsulation layer, (B) a 13-μm-thick base film with a 10-μm-thick encapsulation layer, and (C) a 125-μm-thick base film without an

encapsulation layer. Measurements are performed with applications of V_{DS} = V_{GS} = -40 V. Inset shows the expanded scale from 2 mm to 0 mm.

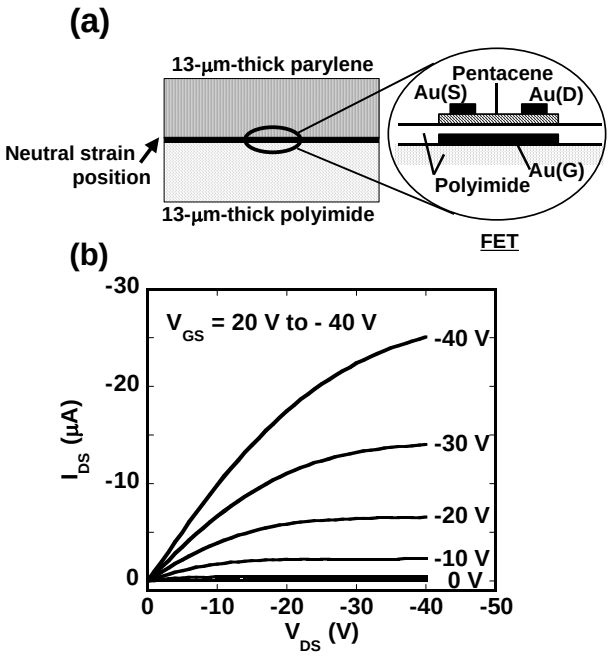

Fig. 1 / Sekitani, *et al*.

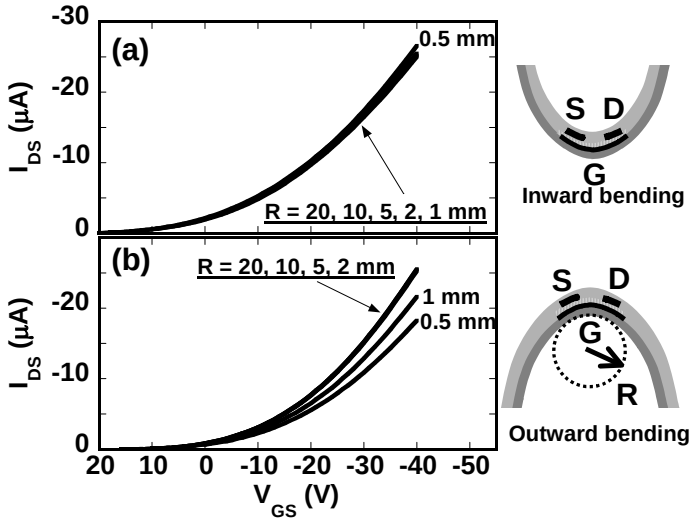

Fig. 2 / Sekitani, *et al*.

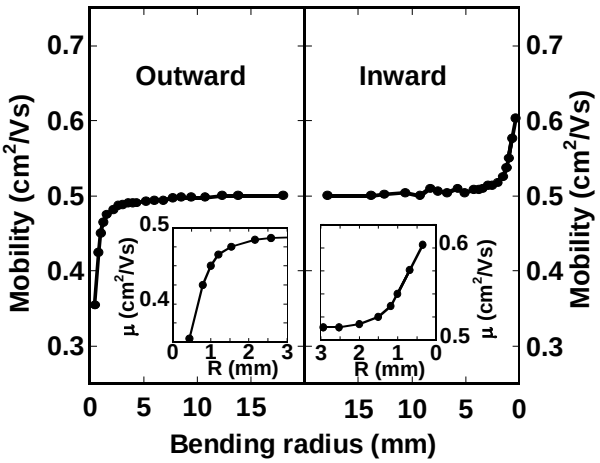

Fig. 3 / Sekitani, *et al*.

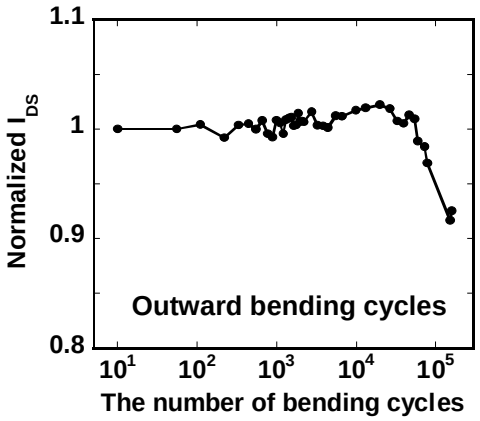

Fig. 4 / Sekitani, *et al*.

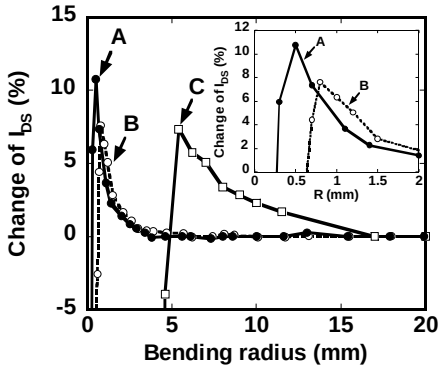

Fig. 5 / Sekitani, *et al*.